

# TRANSVERSE EMITTANCE MEASUREMENT BY SLIT-SCAN METHOD FOR AN SRF PHOTO INJECTOR

P. Lu, H. Vennekate, HZDR & TU Dresden, Germany  
A. Arnold, P. Michel, P. Murcek, J. Teichert, R. Xiang, HZDR, Germany

## Abstract

New measurements of the transverse emittance for a Superconducting Radio Frequency (SRF) gun are conducted with slit-scan method. This contribution introduces the experimental setup, a detailed algorithm and first measurement results. The algorithm proves effective of handling irregular images while the phase space measurement is performed with high resolution. The measured values are around 1-2  $\pi\text{mm}\cdot\text{mrad}$ . The results are compared with ASTRA simulations and quad-scan measurement, followed with analysis about the measurement accuracy.

## INTRODUCTION

An SRF-gun with a 3½-cell cavity has been built up and in commission at Helmholtz-Zentrum Dresden-Rossendorf (HZDR) since 2007. This SRF photo injector is designed to provide an electron beam with the energy of 9.5 MeV and the bunch charge of 1 nC. With different operation modes, it is planned to be use for the infrared free-electron lasers (FELs)[1] and the inverse Compton backscattering research at the radiation source ELBE (Electron Linac with high Brilliance and low Emittance). As a recent performance of the SRF gun, a 3.3 MeV, 30 pC (400  $\mu\text{A}$ ) and 1.6 ps rms bunch length beam has been created to generate the FEL radiation with 50  $\mu\text{m}$  wave length [2].

Transverse emittance plays a significant role on the high bunch charge beam transport. Emittance measurements using solenoid/quadrupole scans and a multi-slits mask have been developed at ELBE [3] and were conducted with the SRF gun [4]. The solenoid/quadrupole scan method does not measure the phase space distribution, while the multi-slits mask method has the difficulty of data overlap between its slits. To solve these problems is the motivation of developing a slit-scan measurement system.

The distinctive feature of this beam diagnostics work is a automatic and universal image processing method with a high tolerance for noises.

## EXPERIMENTAL SETUP

The emittance is measured 2.6 m downstream from the photo cathode, where a 1.5 mm thick tungsten mask with a 0.1 mm wide slit samples the beam. The sampled beamlet is emittance dominated. After about 77 cm of drift, the spread beamlet is recorded by a 45° YAG screen and a CCD camera. If the slit scans all over the beam section, then the complete phase space can be recorded. Fig. 1. illustrates the entire measurement setup.

A labview program is created to control automatically the measurement and computation. For both parts the user-operation time is in seconds but the processing time is around 5 minutes.

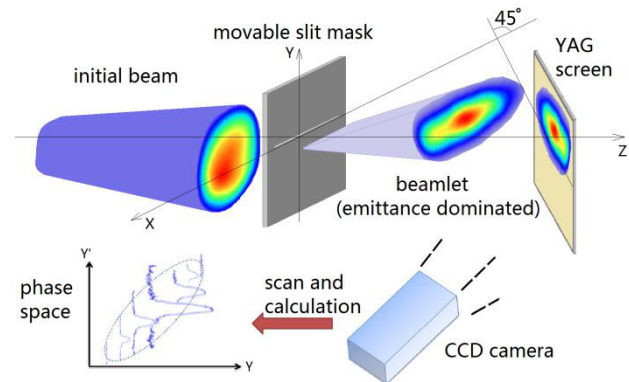


Figure 1: Experimental setup of the slit-scan emittance measurement for the SRF gun at HZDR.

## DATA PROCESSING

Normally, beamlet images from the YAG screen cannot be used directly to obtain the angle distribution. Inevitable background and noisy pixels are common problems [5][6]. In Ref. [5] a Gaussian fit is performed to select the Region Of Interest (ROI), data outside of this area indicates the background and data inside is denoised by an iterative procedure. In Ref. [6] the background is from images of beam-off states. And then the filtering for isolated noises is performed to get a final image.

In our case, a universal and automatic image processing is necessary for the hundreds of images recorded for each measurement. The three main difficulties are listed below and illustrated in Fig. 2.

- Multi-peak beamlet image.
- Weak beamlet signal at the edge of a beam.
- Multi-pixel noises.

For the multi-peak and weak signal cases, universal fittings are usually not accurate enough. And a lot of multi-pixel noises will survive the filtering.

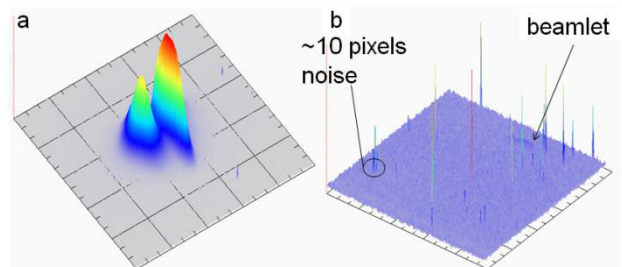


Figure 2: Special cases of beamlet images. (a) multi-peak case. (b) weak-signal case and multi-pixel noise.

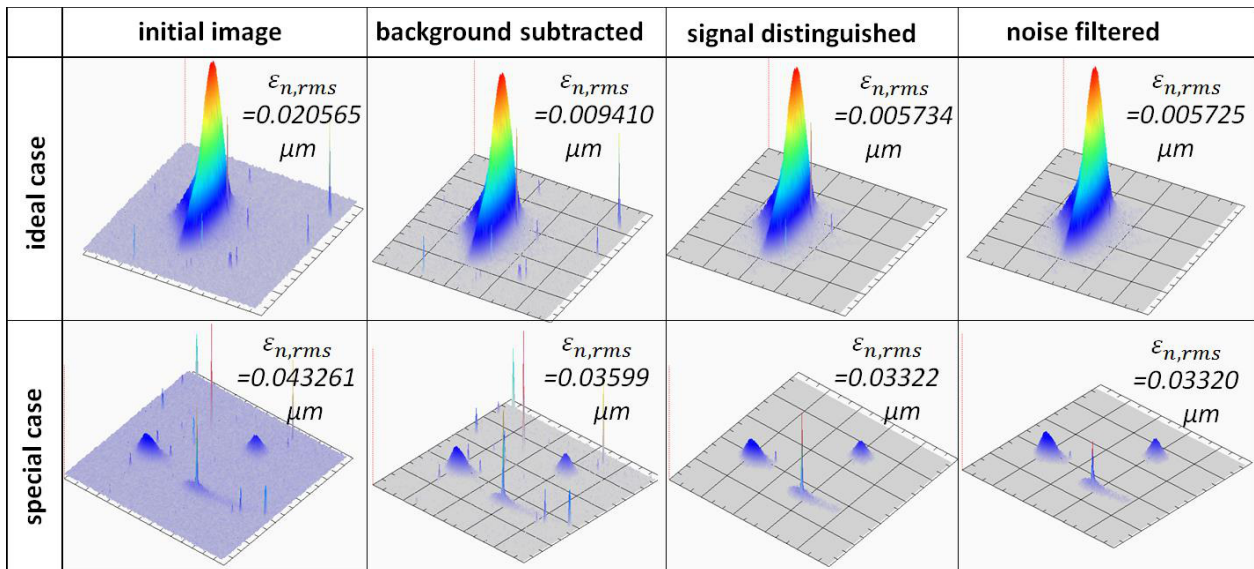


Figure 3: Examples of the image processing algorithm. The  $\epsilon_{n,rms}$  represents for the emittance of the beamlet.

Here we present the procedures of the universal algorithm used in our slit-scan emittance measurement, attempting to process these special cases as well as ideal beamlet images.

- Sum all the valid images to rebuild the beam spot, then choose the ROI manually to exclude pixels outside the screen meanwhile to include the entire beam spot.
- Calculate the background and standard deviation of images taken from the beam-off state. For each valid image, subtract the background and set pixels below the standard deviation to zero.
- Distinguish the beamlet signal and noises. The beamlet signal is defined as “clusters of more than 50 connected none-zero pixels”. Therefore the rest smaller clusters are regarded as noises. All none-zero pixels are grouped to clusters by the steps bellow.
  - Find the next none-zero pixel and create a stack starting with this pixel.
  - Scan the surrounding 8 pixels, add all the undistinguished none-zero pixels into the end of the stack.
  - Repeat the above step with all the elements of the stack, when the stack is traversed, pixels in the stack consist a new cluster.
- Filter the 2D sharp peaks superposed on the distinguished beamlet signal area.

Two examples of both the ideal and the special cases of the beamlet image data processing are shown in Fig. 3. The background subtracting and distinguishing steps have specific criteria so they are completely reliable. For the 2D filtering, the best criteria changes from image to image. However, the beamlet emittance is not sensitive of these unfiltered noises. As shown in the ideal case, the filtering is almost complete and the emittance varies only 2%. Therefore, although the filtering in the special case is

obviously not complete, the error can be assumed to be rather low.

### MEASUREMENTS EXAMPLES

The main advantage of the slit-scan method is the possibility to gain the detailed phase space. In our setup the resolutions of position and angle are respectively 0.1 mm and 0.032 mrad. Examples of measured phase spaces are shown in Fig. 4. The beam energy is 2.43 MeV and the bunch charge is 7.5 pC, (a) shows the phase space of the photoelectron beam and (b) shows the phase space of the weak dark current. Both phase spaces are clear. The asymmetric tail in (a) might be the dark current. In the dark current, two components can be seen and are assumed to be field emission electrons from different positions of the cavity.

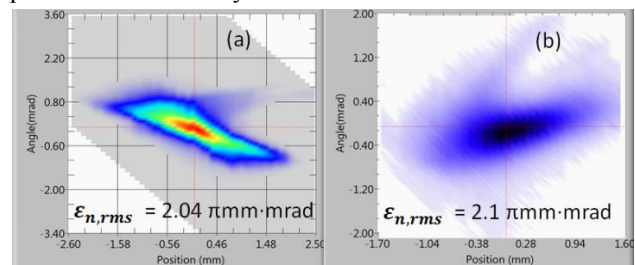


Figure 4: Phase space measurement examples. (a) regular beam phase space, (b) dark current phase space.

In the low bunch charge situation, we measured the emittance with different parameters. The basic beam parameters are 2.43 MeV of energy, 0.05 pC of bunch charge, 30° of laser phase, 5 kV of DC voltage on the cathode and 25 A of solenoid current. The DC voltage is supposed to suppress the multipacting in cavity and the solenoid is installed between the gun exit and the slit position. The bunch charge, DC voltage, laser phase and the solenoid current were scanned to measure the

emittance trend. Simulations using ASTRA are also done for some situations with the same parameters. Results of both are shown in Fig. 5.

For the laser phase scanning, the simulation and the measurement have the same trend, but for the bunch charge scanning and the solenoid scanning, the measured emittance varies more than the simulated values. In general the simulated emittance is larger than the measured. One reason might be that the beamlet signal is too weak and partly buried in the noises [7]. This explains why the emittance between measured and simulated values has a bigger difference for a lower bunch charge.

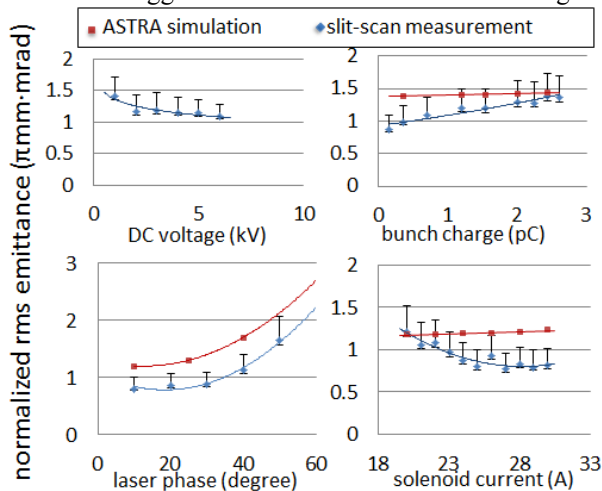


Figure 5: Emittance measurements at low bunch charge.

We also made a comparison with the quad-scan method, with a beam energy of 2.18 MeV and a bunch charge of 0.075 pC. Results are shown in Fig. 6. Both measurements showed the same trend of the emittance vs. solenoid current as in Fig. 5, but the slit-scan data are again smaller. We did the correction in Ref. [7] by multiplying the emittance with a correction factor. The correction factor is the ratio of the measured the beam size without the slit mask and the calculated beam size from beamlet signals. With lower solenoid current, the corrected slit-scan results match the quad-scan results. Nevertheless, in case the solenoid current exceeds 23 A, the correction factor is extremely high which cannot be explained at the moment. Further investigations are necessary to elaborate on this topic.

Furthermore, both the simulation and the quad-scan emittance measurement method have their own uncertainty, which is not discussed in this paper.

## MEASUREMENT ACCURACY

For the well-matched correction cases in Fig. 6, the correction factor is about 1.20. Therefore, we can assume a systematic error of about +20% due to the weak sampled signal effect. For the basic setup of a 45° YAG screen, an error of +3% is estimated [8]. As mentioned above, we believe the data processing error is less than 2%. The camera installation error and the electronics error are estimated to be less than 3%. The error bars in Fig. 5.

and Fig. 6. sum of these errors only. Other uncertainties such as the beam instability demand further study.

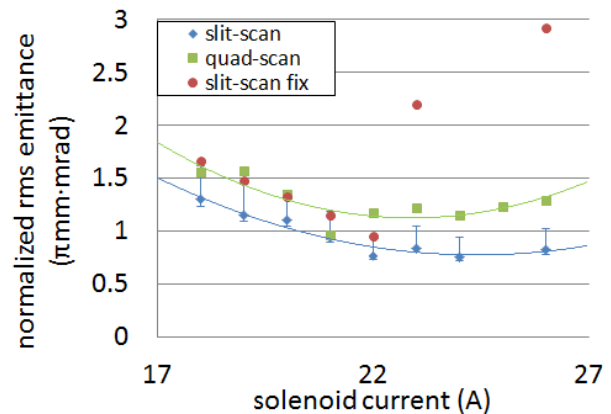


Figure 6: Comparison with the quad-scan method.

## CONCLUSION

In this slit-scan emittance measurement, we try to avoid any fitting in image processing. A reliable algorithm is developed to separate the beamlet signal from noisy backgrounds. However, some of the sampled beamlet is too weak to be detected. This causes the main error of up to 20%. Nevertheless, this method is still effective in measuring the high-resolution beam phase space.

## ACKNOWLEDGEMENT

We acknowledge the support of the European Community-Research Infrastructure Activity under the FP7 programme (EuCARD, contract number 227579), as well as the support of the German Federal Ministry of Education and Research grant 05 ES4BR1/8, and the LA<sup>3</sup>NET funding from the European Commission under Grant Agreement Number GA-ITN-2011-289191.

## REFERENCES

- [1] W. Seidel, et al. Proceedings of FEL08, Gyeongju, Korea, 2008, p. 382.
- [2] J. Teichert, et al. Free-Electron Laser Operation with a Superconducting Radio-Frequency Photoinjector at ELBE, submitted to FEL2013 proceedings
- [3] P. Evtushenko, Ph.D. thesis, Technical University Dresden, 2004.
- [4] T. Kamps, et al. Rev. Sci. Instrum. 79, 093301 (2008).
- [5] A. Mostacci, et al. Rev. Sci. Instrum. 79, 013303 (2008).
- [6] Lazar Staykov, Ph.D. thesis, University of Hamburg, 2008.
- [7] F. Stephan, Normal-conducting RF Photo Injectors for Free Electron Lasers, report at First Topical Workshop on Laser Particle Sources, 2013.
- [8] Martin Schmeißer, Emittance Measurements of a Superconducting High Frequency Electron Gun, Forschungsbeleg of HZB, 2013